Magnetic structure of ground and field-induced ordered states of low-dimensional α-CoV_2O_6: Experiment and theory

M. Lenertz, J. Alaria,* D. Stoeffler, S. Colis,† and A. Dinia
Institut de Physique et Chimie des Matériaux de Strasbourg (IPCMS), UMR 7504 CNRS and Université de Strasbourg (UDS-ECPM), 23 rue du Loess, BP 43, F-67034 Strasbourg Cedex 2, France

O. Mentré
Université Lille Nord de France, UMR 8181 CNRS, Unité de Catalyse et de Chimie du Solide (UCCS USTL), F-59655 Villeneuve d'Ascq, France

G. André and F. Porcher
CEA, Centre de Saclay, DSM/IRAMIS, Laboratoire Léon Brillouin (LLB), F-91191 Gif-sur-Yvette, France

E. Suard
Institut Max von Laue-Paul Langevin (ILL), 6 rue Jules Horowitz, BP 156, F-38042 Grenoble Cedex 9, France
(Received 19 September 2012; published 28 December 2012)

In this work, we investigate the magnetic properties of the monoclinic α-CoV_2O_6 by powder neutron diffraction measurements and *ab initio* calculations. An emphasis has been pointed towards the magnetic structure and the interaction between the Co ions leading to magnetic frustrations in this compound. Neutron diffraction experiments were carried out both in the ground state (zero magnetic field) and under applied external field of 2.5 and 5 T corresponding to the ferrimagnetic and ferromagnetic states, respectively. The antiferromagnetic ground state below 14 K corresponds to $k = (1,0,\frac{1}{2})$ magnetic propagation vector in $C1$ space group. The magnetic structure can be described by ferromagnetic interactions along the chains (b axis) and antiferromagnetic coupling between the chains (along a and c axes). The ferrimagnetic structure implies a ninefold unit cell (3a, b, 3c) in which ferromagnetic chains follow an "up-up-down" sequence along the a and c axes. In the ferromagnetic state, the spin orientations remain unchanged while every chain lies ferromagnetically ordered. In all cases, the magnetic moments lie in the ac plane, along the CoO_6 octahedra axis, at an angle of 9.3° with respect to the c axis. The magnetic structure of α-CoV_2O_6 resolved for all the ordered states is successfully related to a theoretical model. *Ab initio* calculations allowed us to (i) confirm the ground-state magnetic structure, (ii) calculate the interactions between the Co ions, (iii) explain the frustration leading to the stepped variation of the magnetization curves, (iv) calculate the orbital magnetic moment (1.5 μ_B) on Co atoms, and (v) confirm the direction of the magnetic moments near the c direction.

DOI: 10.1103/PhysRevB.86.214428 PACS number(s): 75.47.Lx, 75.30.−m, 61.05.fm

I. INTRODUCTION

Low-dimensional magnetic oxides are a subject of increasing attention from the scientific community due to their peculiar properties such as the strong anisotropy or the step magnetization reversal.[1–3] An additional interest for this system is the presence of different magnetic configurations that are related to different resistive states[1] in the same manner as this is usually observed in magnetic tunnel junction systems.[4] Therefore, such materials can be also used as model systems for the study of magnetoresistive properties as no roughness or diffusion usually observed in magnetic tunnel junctions at the magnetic/nonmagnetic interfaces is allowed. The existence of the magnetization plateaux is often explained on the basis of triangular frustrated Ising-type spin system.[2] However, in the case of nontriangular (or hexagonal) systems, the origin of the magnetization steps is much less trivial.

CoV_2O_6 is a one-dimensional magnetic oxide that exhibits two allotropic phases: a triclinic phase called γ-CoV_2O_6,[5] and a monoclinic one called α-CoV_2O_6.[3,6,7] Both phases in polycrystalline form have been recently studied in our group, but no strong proof of the magnetic ordering could be obtained.[8] The presence of magnetization plateaux is evidenced in both phases, thus suggesting the existence of magnetic frustrations. However, the relative orientation of the magnetic moments was a subject of intense investigation. The existence of the magnetization steps in the MH curves along with the temperature dependence variation of the magnetization only suggests the existence of antiferromagnetic (AF) interactions (assumed between the chains) and ferromagnetic (F) interactions (assumed inside the chains) (see, e.g., Refs. 3 and 8). More recently, neutron diffraction studies were carried out on the γ- and α-CoV_2O_6 phases. In γ-CoV_2O_6, these measurements showed the existence of a ($\frac{1}{2}$, 0, 0) magnetic propagation vector which suggests that the interactions are AF and F along the a and c axes, respectively, but were unable to show unambiguously the ferromagnetic order inside the chains (i.e., along the b axis).[9] This is mainly due to the fact that along the chains, the γ phase contains two independent Co sites which are not perfectly aligned but show angles different of 180°. In contrast, for α-CoV_2O_6, both the ground[10] and field-induced[11] states magnetic structures were determined by neutron diffraction on polycrystalline samples. It is shown unambiguously that the magnetic moments lie in the ac plane and are coupled within the chains of edge-sharing

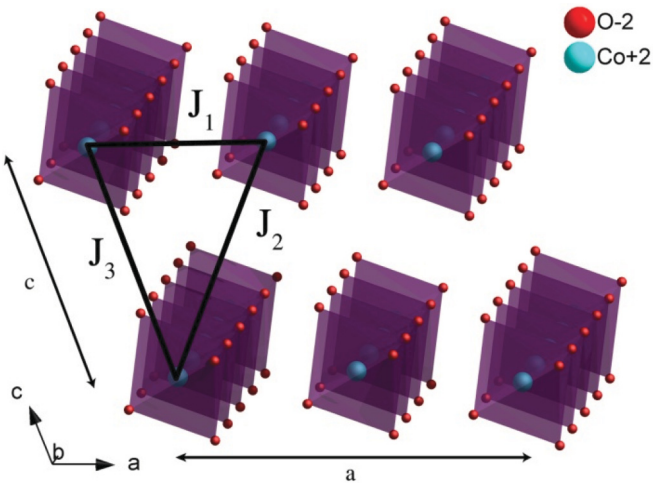

FIG. 1. (Color online) Crystalline structure of α-CoV_2O_6. Only the Co chains constituted of CoO_6 octahedra have been represented for visibility reasons. The VO_6 octahedra (not represented) are located in the *ab* plane (Ref. 8). The J_i couplings represent the magnetic interactions between chains as reported by Yao (Ref. 12).

Co^{2+} octahedra running parallel to the *b* axis. According to the refinements of the neutron diffraction data, the magnetic moments in the ground state are nearly perpendicular to the *a* axis and quite far from the *c* axis.[10] Moreover, this orientation changes in the field-induced (ferrimagnetic and ferromagnetic) structures.[11] This observation is, however, peculiar if we keep in mind that the easy magnetization axis is along (or very close to) the *c* direction as clearly evidenced in α-CoV_2O_6 single crystals.[3]

From the theoretical point of view, two main models aiming to describe the magnetic interactions and therefore the frustrations leading to the magnetization plateaux in α-CoV_2O_6 are reported. The model of Yao[12] shows, using Wang-Landau simulations, that although the crystalline structure of α-CoV_2O_6 is not constituted of regular triangles, the magnetization steps can be explained in terms of frustrations between the chains in the *ac* plane (Fig. 1). Because it considers the interactions between chains and not between individual atoms, this model is in disagreement with the magnetic structure expected for this compound suggested by the neutron diffraction data.[11] The more recent model of Kim *et al.*[13] shows, using *ab initio* calculations, that the magnetization plateaux can be also obtained if we consider the interactions between individual Co ions and not between chains. The model estimates also the ratio between the different considered interactions, nevertheless, without giving absolute values of these interactions.

In this paper, we will focus on this same monoclinic α-CoV_2O_6 phase which exhibits a brannerite structure. As briefly mentioned, this structure contains edge-sharing CoO_6 octahedra forming one-dimensional chains along the *b* axis. In the *ab* plane, the chains form magnetic planes and in the *c* direction the CoO_6 chains are separated by nonmagnetic VO_6-based layers. At 5 K, α-CoV_2O_6 exhibits a steplike magnetization curve with a step at $\frac{1}{3}$ of saturation magnetization. With respect to the γ phase, the Co ions are perfectly aligned inside the chains and the magnetization plateaux are much better defined.[8]

In this context, our paper aims to shed a coherent light on the magnetic properties of α-CoV_2O_6 and clarify some existing discrepancies between the experimental and/or theoretical results. The magnetic structure of α-CoV_2O_6 in the ground state and upon an increasing external field is reported with an emphasis on the angle existing between the magnetic moments and the *c* axis (i.e., easy magnetization axis). We also propose a model based on *ab initio* calculations that considers interactions between individual atoms to support the magnetic structure refined from neutron diffraction data. The calculations give an estimation of the magnetic interactions which are compared to those given by the model of Yao[12] and to the switching fields experimentally estimated from low-temperature magnetization measurements.[3,8] Preliminary results taking into account the spin-orbit coupling suggest that the magnetic moments are oriented along the CoO_6 octahedra axis, close to the *c* axis, in agreement with our neutron diffraction data and the anisotropy results reported in literature on single crystals.[3] Moreover, our calculations also show that the orbital magnetic moment per Co atom is 1.5 μ_B, in good agreement with the experimental results. Finally, this paper gives a unified picture of the α-CoV_2O_6 magnetic properties using both neutron diffraction measurements and theoretical calculations.

II. EXPERIMENTAL DETAILS

The polycrystalline α-CoV_2O_6 powder was prepared by solid-state reaction from vanadium oxide and hydrated cobalt oxalate. Both compounds were ground together in agate mortar and then heated during 40 h at 720 °C in a platinum crucible. The resulting powder was ground in order to obtain a fine powder. Stoichiometry was checked by energy dispersive x-ray spectrometry (EDS) analysis and showed a good agreement between the measured and the nominal values. The magnetic properties were analyzed using a MPMS SQUID-VSM (Quantum Design) magnetometer. The measurements were carried out in two configurations. In one case, the polycrystalline powder was magnetically "aligned" in a polymeric gel that freezes the particle orientation below about 35 °C. The alignment was performed in a field of 7 T. The purpose of this measurement is to allow a direct comparison with the magnetization curves reported in literature on α-CoV_2O_6 single crystals. In the second case, the powder (random crystallite orientation) was measured directly, without any previous magnetic alignment treatment. The aim of this measurement is to give an image of the magnetization status of the powder at 2.5 and 5 T in the same conditions (random crystallite orientation) as those obtained during the field-dependent neutron diffraction measurements.

Zero-field neutron diffraction measurements were performed at the LLB facility at Saclay (France) using the 3T2 high-resolution powder diffractometer with a 0.1225-nm wavelength and the G4.1 two-axis diffractometer equipped with a cryostat and using a 0.2423-nm wavelength. Using the 3T2 instrument, the accurate nuclear structure was refined while the G4.1 instrument was used to determine the magnetic structure in the ground state at 1.5 K and the evolution of

this structure as a function of temperature. Neutron diffraction under magnetic field was carried out at the ILL facility at Grenoble (France) using the D2B diffractometer (0.2399-nm wavelength) equipped with a cryomagnet delivering a magnetic field up to 5 T which enables the determination of both the ferrimagnetic and ferromagnetic states. For all measurements, the sample was placed in a 8-mm diameter vanadium can. For the measurements under magnetic field, the sample was pressed in order to limit the powder reorientation under high magnetic fields. Because of the weak V atoms scattering length for neutrons, the atomic position of V has been refined using x-ray diffraction (XRD) data. The XRD measurements were carried out on a D8 Brücker-AXS diffractometer (Cu $K\alpha_1$ wavelength $\lambda = 0.154\,056$ nm) and equipped with a front monochromator. The diffracted beam was energy filtered in order to eliminate the fluorescence background.

III. RESULTS AND DISCUSSION

Figure 2 shows field-dependent magnetic properties. For the magnetically "aligned" sample, the antiferromagnetic ground state is well distinguished in the MH curve recorded at 5 K as for fields smaller than $H_{c1} = 1.5$ T, the magnetization is negligible. This is in agreement with the temperature-dependent magnetic measurements (not shown here) which indicated an antiferromagnetic state with a Néel temperature of 14 K.[7,8] Above H_{c1}, the magnetization increases and reaches a value corresponding to $\frac{1}{3}$ of the saturation magnetization which has been correlated to possible magnetic frustrations. By further increasing the field, a second magnetization step is observed around $H_{c2} = 3.5$ T. Complete saturation is reached above 4.5 T. The magnetic moment is about 4.6 μ_B/Co, much larger than the expected value of 3 μ_B/Co (high spin Co^{2+} in octahedral environment), and suggests the existence of a strong spin-orbit coupling in this compound. The existence of the magnetization plateaux and of the strong anisotropy as reported in α-CoV_2O_6 single crystals[3,7] is also compatible with the existence of ferromagnetic correlation inside the chains. It is interesting to point out that in the magnetically random samples, no well-defined plateaux can be observed in the MH curve typical of the uniaxial behavior of the grains toward the magnetic field. While the antiferromagnetic ground state is still present, the magnetization transitions at 1.5 and 3.5 T are very smooth and, consequently, the magnetization values for magnetization plateau and saturation are not reached anymore. At 7 T, the magnetization is only about 2.35 μ_B/Co ion, i.e. about 50% of the expected value. This is due to the extremely strong magnetic anisotropy[3] and to the random orientation of the easy magnetization axis (i.e., the c axis) of the particles.

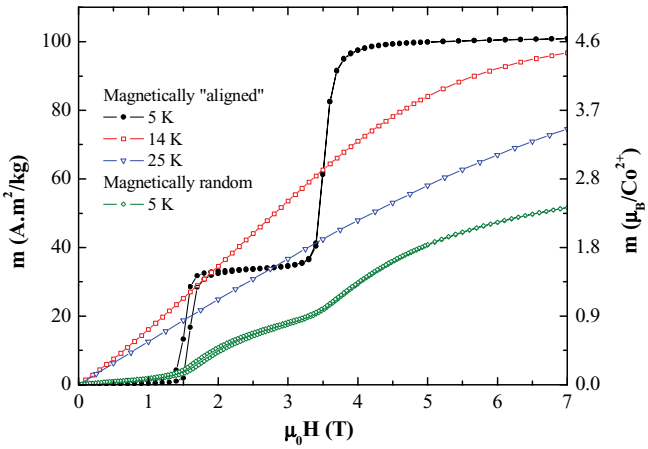

FIG. 2. (Color online) Magnetization curves for the magnetically "aligned" sample recorded at 5, 14, and 25 K. At 5 K, the magnetization plateaux are well evidenced. A magnetization curve at 5 K for a magnetically random sample is also given for comparison.

Figure 3 shows some of the neutron diffraction patterns fitted using the Rietveld method using the FULLPROF software. The Thompson-Cox-Hastings pseudo-Voigt convoluted with axial divergence asymmetry profile function was used for modeling the diffraction peaks. The background was modeled by linear interpolation between particular points. Anisotropic atomic displacement parameters were considered. The March's function was also used for correction of the preferred orientations along the b crystallographic axis. This preferred orientation strongly affects our x-ray diffraction data and remain present in the neutron diffraction patterns probably due to the sample pressing. It is striking that these corrections appear necessary for a good matching between experimental and calculated patterns. Under a magnetic field, a second set of preferred orientations along the c axis was also considered to reproduce the sample reorientation along with a magnetic field. In details, in order to correct these effects with comparable importance in the several collected patterns, primary neutron diffraction data were collected at 25 K before and after applying a field of 5 T to model each elementary contribution to the preferred orientations. Note that after applying once the 5-T magnetic field, the orientation of the crystallites in the field did not show further changes upon changing the field. Table I shows the reliability factor (R) for the neutron diffraction measurements. Tables II and III show the cell parameters of α-CoV_2O_6 at different temperatures (1.5, 25, and 300 K) and the atoms positions refined at 300 K. No Co/V site disorder similar to the Mn/V one reported for the isostructural MnV_2O_6 compound[14] could be observed. Note that the position of the V ion could not be refined from the neutron diffraction data. From the x-ray diffraction data, the V position was refined while keeping fixed the position of the other atoms at the values calculated from the neutron diffraction data.

The neutron diffraction measurements recorded at different temperatures (Fig. 3 and Table II) did not show evidence of phase transition upon cooling, consistent with results given in Ref. 10. Below 14 K, significant magnetic satellites appear that can be indexed either with a $k = (1,0,\frac{1}{2})$ propagation vector using a C-centered lattice or with a $k = (0,0,\frac{1}{2})$ using a primitive lattice. The key point behind these two equivalent solutions is the spin reversal following the C-centering translation inside the elementary cell. After final refinement, the magnetic structure shows Co atoms ferromagnetically coupled along the chains (i.e., the b direction) and antiferromagnetically coupled between adjacent chains [along a and c; see Fig. 4(a)], in agreement with the antiferromagnetic ground state reported by Markkula *et al.*[10] The refined magnetic moment on Co atoms is 4.09(3) μ_B and lies in the ac plane, near the c direction, along

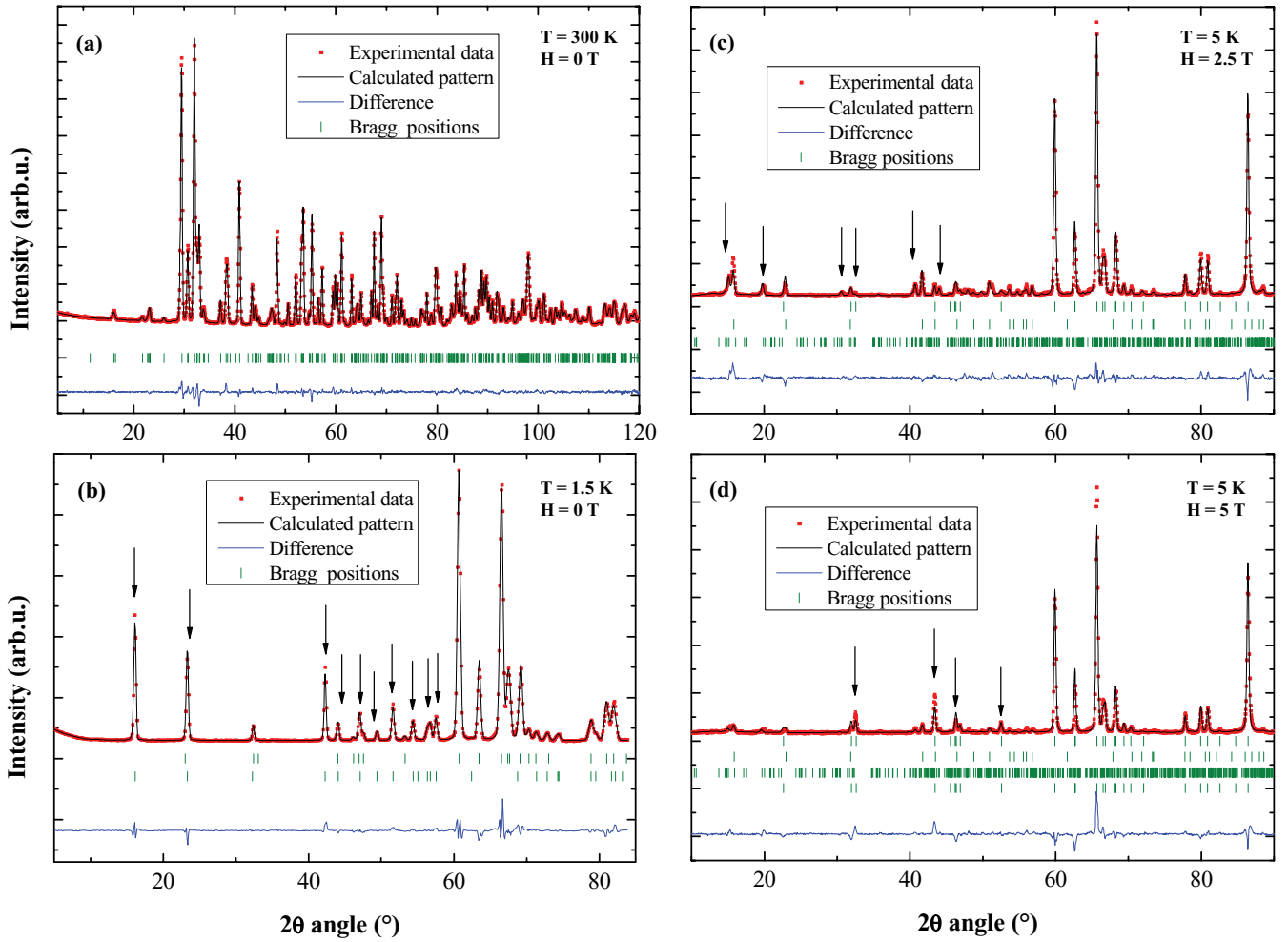

FIG. 3. (Color online) Zero-field neutron diffraction patterns for α-CoV_2O_6 at (a) room temperature (3T2: $\lambda = 0.1225$ nm) and (b) 1.5 K (G4.1: $\lambda = 0.2423$ nm). Neutron diffraction patterns recorded at (c) 5 K and 2.5 T corresponding to the ferrimagnetic state, and (d) 5 K and 5 T corresponding to the ferromagnetic state (D2B: $\lambda = 0.2399$ nm). Red: experimental data, black: the calculated pattern, blue: the difference, and green: the Bragg positions. The arrows in (b), (c), and (d) show the main antiferromagnetic, ferrimagnetic, and ferromagnetic peaks, respectively.

one of O-Co-O directions of the CoO_6 octahedron (Fig. 4), and which is also the easy magnetization axis. The angles between the magnetic moment and the a and c axes are of 121.4(4)° and 9.3(4)°, respectively. The projections of the magnetic moment along the a and c axes are of $-0.72(3)\ \mu_B$ and $3.77(3)\ \mu_B$. Along the c direction, the Co-O length is shorter [1.975(1) Å] than along the other directions [2.200(1) Å]. It is interesting to point out that the same ground-state structure was also found for the isostructural MnV_2O_6 compound,[14] although this compound shows no magnetization plateaux in the *MH* curves. Note also that comparing to neutron diffraction patterns recorded on γ-CoV_2O_6 powders,[9] in our case all

TABLE I. Reliability factors (R) of the neutron diffraction data recorded on α-CoV_2O_6 and shown in Fig. 3. The ratio of the antiferromagnetic, ferrimagnetic, and ferromagnetic phases in the sample is also reported.

Field /Temp./Instrument	Antiferromagnetic state		Ferrimagnetic state		Ferromagnetic state		Nuclear
T/K	Ratio	Mag. R (%)	Ratio	Mag. R (%)	Ratio	Mag. R (%)	Bragg R (%)
0/300/3T2							3.06
0/25/G4.1[a]							3.72
0/1.5/G4.1	1	4.78	0		0		4.20
0/5/D2B[a]	1	13.5	0		0		7.58
2.5/5/D2B	0.54	21.1	0.46	23.6	0		7.88
5/5/D2B	0.20	23.3	0.14	37.2	0.66	26.4	13.7

[a]Pattern not presented here.

TABLE II. α-CoV_2O_6 lattice parameters refined from the neutron diffraction patterns recorded at different temperatures.

Temperature	300 K (3T2)	25 K (G4.1)[a]	1.5 K (G4.1)
a (Å)	9.25449(7)	9.2341(8)	9.250(2)
b (Å)	3.50444(2)	3.5052(4)	3.5101(8)
c (Å)	6.62081(5)	6.6026(6)	6.613(2)
α (deg.)	90	90	90
β (deg.)	111.6278(5)	112.046(3)	112.067(3)
γ (deg.)	90	90	90

[a]Pattern not presented here.

peaks (even the small-angle ones) could be refined. For γ-CoV_2O_6, these reflexions were attributed to long-wavelength modulations of the magnetic structure[9] as the ones observed in $Ca_3Co_2O_6$.[15,16] Our results suggest that no such phenomena occur in α-CoV_2O_6.

For the neutron diffraction measurements under magnetic field, because of the preferred orientations, the values of the magnetic moments and their directions were kept fixed to the previously determined values (measurements without field). When applying a magnetic field of 2.5 T, new magnetic peaks are observed [Fig. 3(c)]. These peaks can be indexed using a propagation vector $k = (\frac{2}{3},0,\frac{1}{3})$ in the $C1$ space group and correspond to an "up-up-down" configuration of the Co magnetic moments of the chains along the a and c directions [see Fig. 4(b)]. This propagation vector generates an antiferromagnetic structure with nonequivalent moments on Co atoms along the a direction, i.e., M_{up}, $M/2_{down}$, $M/2_{down}$, inconsistent with the ferrimagnetic state. It is why a ninefold unit cell (3a, b, 3c) was used with no propagation vector in the $P1$ space group in which elementary magnetic moments were manually placed and strained together according to the sequence of spin orientations obtained using the antiferromagnetic $k = (\frac{2}{3},0,\frac{1}{3})$ vector. This configuration is in agreement with previous results[7,10,12] and with the $\frac{1}{3}$ of the saturation plateau observed by SQUID measurement on the magnetically "aligned" powder. Note that although at 2.5 T an oriented sample should be in a ferrimagnetic state, a significant amount of antiferromagnetic [$k = (1,0,\frac{1}{2})$] powder is still observed in the neutron diffraction pattern. The amount of each magnetic phase was quantified and shown in Table I. 46% of the sample was found to be in ferrimagnetic state suggesting that the sample magnetization is only about 15% of the saturation value. This is in agreement with the MH measurement carried out on the magnetically random sample (Fig. 2) which shows a smaller magnetization than that of the "aligned" sample, i.e., about 15% of the saturation value at $H = 2.5$ T. Rising the magnetic field up to 5 T, further new contributions grow up on the nuclear Bragg peaks [Fig. 3(d)], typical of a ferromagnetic structure. As in the case of the pattern recorded at 2.5 T, the fit of the pattern recorded at 5 T requires the concomitant presence of the three antiferromagnetic, ferrimagnetic, and ferromagnetic states defined above. Note that when progressively increasing the field, the intensities of the lines corresponding to the ground antiferromagnetic state decrease, leading to 20%, 14%, and 66% for the antiferromagnetic, ferrimagnetic, and ferromagnetic fractions, respectively. This corresponds to about 70% of the saturation magnetization. As in the case of the SQUID MH curves on the magnetically random samples, the sample magnetization is only at 40% of saturation. This difference can be attributed to an overestimation of the amount of the ferromagnetic phase due to preferred orientation of the magnetic phases at larger fields. Moreover, the presence of multiple magnetic phases can be explained by the strong anisotropy of α-CoV_2O_6. The distribution of the easy magnetization axes induces a different probability to switch different crystallites from one magnetic state to another. As a consequence, each magnetic phase has its own preferred orientation and therefore it is difficult to accurately determine the proportion of each magnetic phase using neutron powder diffraction. For this purpose, measurement on single crystals is necessary.

TABLE III. Refined atomic coordinates in α-CoV_2O_6 as calculated from the neutron diffraction data recorded at 300 K. The coordinate of V was fixed to the value obtained from the refinement of the XRD data.

Atom	x	y	z
Co	0.0	0.0	0.0
V	0.194(3)	0.0	0.155(4)
O1	0.0356(1)	0.0	0.2237(2)
O2	0.3469(2)	0.0	0.3900(2)
O3	0.6924(1)	0.0	0.0653(2)

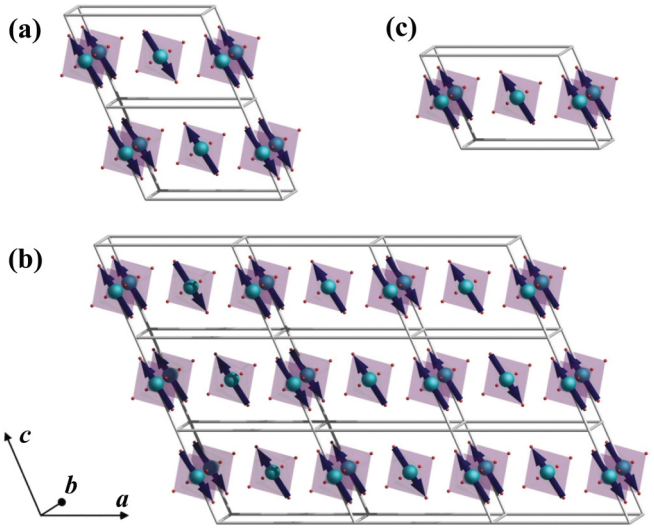

FIG. 4. (Color online) Magnetic structure of α-CoV_2O_6 (a) in the antiferromagnetic ground state [propagation vector $k = (1,0,\frac{1}{2})$], (b) in the ferrimagnetic state [ninefold unit cell (3a, b, 3c)], and (c) in the ferromagnetic state. The propagation vectors are considered in the $C1$ space group. The interaction between the Co atoms is ferromagnetic and the moments are always (almost) parallel along the c axis. Co atoms are in blue and O1 and O2 are in red. O3 and V atoms are not shown for visibility reasons. The blue arrows indicate the direction of the magnetic moments.

In order to have information on the position of the V atom, x-ray diffraction patterns of α-CoV_2O_6 were recorded and reported in Fig. 5. All peaks correspond to the α phase and

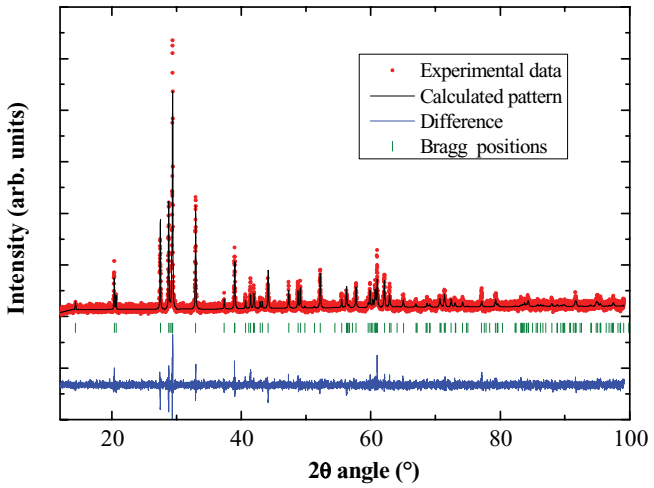

FIG. 5. (Color online) X-ray diffraction pattern for α-CoV_2O_6 at room temperature ($\lambda = 0.154\,056$ nm). Red: experimental data, black: the calculated pattern, blue: the difference, and green: the Bragg positions.

can be indexed using the $C2/m$ (12) space group.[7,17] As in the case of neutron diffraction, no traces of spurious phases could be detected. The pattern could be refined using the Rietveld method. The values of the lattice parameters (similar to those obtained by neutron diffraction) match the values previously reported in literature. By keeping fixed the atomic positions of Co and O, the refinement allowed obtaining information on the position of the V ion, otherwise invisible to neutron due to its low scattering length. This position [0.194(3), 0, 0.155(4)] is reported in Table III.

In order to understand the origin of the plateaux in the *MH* curve in α-CoV_2O_6, Yao[12] developed a model using Wang-Landau simulation and based on irregular triangle interactions. The structure is assumed to be composed of CoO_6 chains ferromagnetically ordered along the b direction. In Yao's model, only positive interactions J_i between the chains are considered. The interactions into competition are consequently only considered in the irregular triangles in the ac plane (Fig. 1). In such case, the distances between the chains are equal to $c = 6.621$ Å along J_3 and $d = 6.532$ Å along J_2. For this reason Yao takes J_2 larger than J_3 so that the arrangement is antiferromagnetic along the J_2 coupling and ferromagnetic along the J_3 one (J_1 is the strongest interaction and corresponds to the shortest distance of 4.948 Å). This configuration corresponds to a $k = (1,0,0)$ propagation vector in the $C1$ space group (antiferromagnetic relation between the two Co atoms of the unit cell). However, if we consider the interaction between the atoms j_1, j_2, and j_3 instead of the interactions between chains (J_i), the Co-Co distance corresponding to j_2 becomes 6.763 Å while that along j_3 does not change. If we keep the assumption that the coupling values are proportional to the Co-Co distances, j_2 coupling becomes weaker with respect to j_3. Therefore, the Co atoms are antiferromagnetically organized along c and ferromagnetically organized in the direction of the j_2 coupling. This situation corresponds to the one calculated from the neutron diffraction data.

To determine the j_i couplings within the model considering the interaction between atoms, we have calculated the total

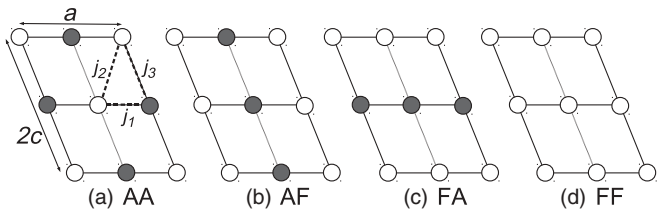

FIG. 6. Schematic representation of the (ac) plane magnetic orderings considered: (a) AA where the j_2 coupling is frustrated, (b) AF where the j_3 coupling is frustrated, (c) FA where the j_1 coupling is frustrated, and (d) FF where all couplings are frustrated.

energy of various magnetic configurations into a supercell using a first-principles density functional theory method. For the considered systems, the band structure is self-consistently calculated using the full potential linearized augmented plane wave (FLAPW) method in the FLEUR implementation[18] using the generalized gradient approximation (GGA) with the Hubbard contribution (GGA + U) and taking core, semicore, and valence states into account. This well-established method has been successfully used in the past for investigating such kinds of oxides.[19–21] For the GGA + U method, we set U_{Co} equal to 5 eV, which is the usual value found in the literature and we set $U = 0$ for all other atoms. The present calculations do not include the spin-orbit coupling and only spin magnetic moments are considered. We have nevertheless checked that, when the same quantization axis is used, the total-energy differences between various magnetic solutions into the two formula unit (f.u.) cells are not changed when taking the spin-orbit coupling into account.[22] All calculations are carried out for a set of increasing **k** points (96 and 736) until no variation into the main results is reached. Finally, the densities of states (DOS) are calculated using also 736 **k** points. The used supercell is built by doubling the $C2/m$ unit cell (containing two formula units) into the c direction. This supercell contains four Co atoms into the ac plane and allows us to consider four different magnetic orders which are identified by the nature of the magnetic arrangement into the a and c directions: A for alternating (positive and negative) successive magnetic moments and F when all moments have the same sign (see Fig. 6).

Because the magnetic interactions between the Co atoms are weak, the atom projected densities of states are very similar and the magnitude of the Co magnetic moment is 2.70 μ_B for all various magnetic configurations considered here (justifying *a posteriori* the use of an Ising model). For the FF solution, the total spin magnetic moment is equal to 3 μ_B per Co atom. Figure 7 displays the densities of states obtained for this FF configuration. Whatever the magnetic configuration is, these DOS confirm (i) the weak overlap between the Co and the V states and (ii) the insulating character of the system with a band gap around 1.9 eV. A very satisfactory point is that the ground state corresponds to the AA configuration in agreement with experiment: this result is not trivial because the cell is large and the interactions are weak. The AF and FA solutions have similar energies and, as expected, the FF solution is the less stable.

In order to determine the j_i couplings, we use the equivalent expression for the Ising Hamiltonian as that of Yao[12]:

$$\mathcal{H} = \sum_{(i,j)} j_{ij} S_i S_j - HM \qquad (1)$$

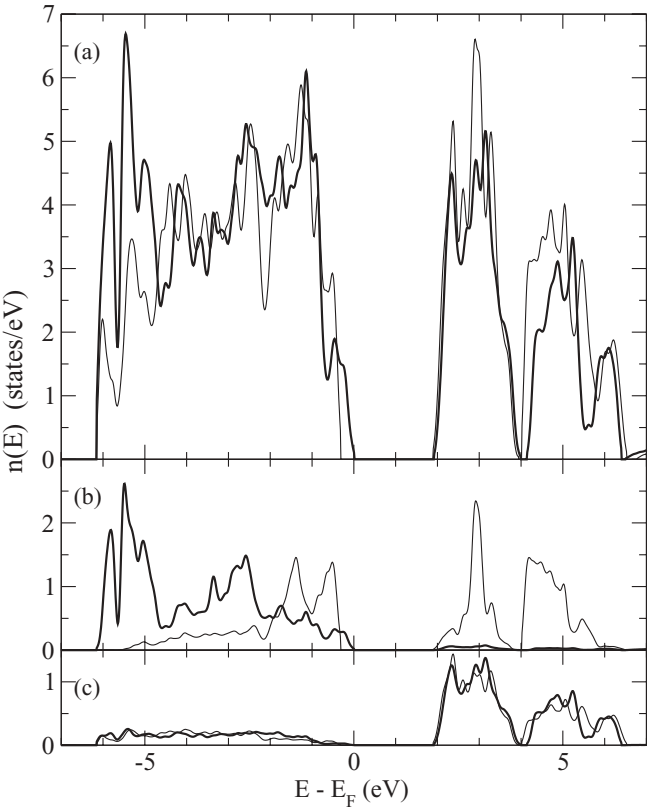

FIG. 7. Total and atom projected densities of states (DOS) obtained for the FF magnetic configuration: (a) total DOS, (b) Co projected DOS, and (c) V projected DOS. The majority (and minority) spin DOS was represented using a thick (thin) line.

(with H the applied field and M the total magnetization) where we consider pairs (i, j) of Co atoms and not chains. For $H = 0$, the total energies calculated using the *ab initio* method can be written as a function of the j_i couplings introduced previously (Table IV).

By solving the equations in j_i we get $j_1 = 0.356$ meV, $j_2 = 0.051$ meV, and $j_3 = 0.463$ meV. Surprisingly, j_1 and j_3 are comparable and j_2 is seven to nine times smaller. This confirms that the distance gives only an indication of the strength of the couplings. The two critical magnetic fields where the plateaux occur can be determined assuming that the calculated couplings give the energy of the $M_S/3$ state where the magnetic moments are ordered up/up/down along the three couplings $[E_{\text{Ising}}(M_S/3) = -(2j_1 + 2j_2 + j_3)/3]$; with the small supercell used in this work for the electronic-structure calculations, it is not possible to build the $M_S/3$ configuration in order to get $E_{\text{ES}}(M_S/3)$. We get the same expressions as Yao[12] where $J_1 = 2j_1$, $J_2 = 2j_2$, and $J_3 = j_3$:

$$H_{c1} = 3[E_{\text{Ising}}(M_S/3) - E_{\text{Ising}}(AA)] = 2(2j_1 - 4j_2 + j_3), \tag{2}$$

$$H_{c2} = 3[E_{\text{Ising}}(FF) - E_{\text{Ising}}(M_S/3)]/2 = 2(2j_1 + 2j_2 + j_3), \tag{3}$$

and

$$H_{c2}/H_{c1} = (1 + r)/(1 - 2r) \tag{4}$$

with $r = 2j_2/(2j_1 + j_3)$. Using the couplings obtained previously, we get $r = 0.087$ and $H_{c2}/H_{c1} = 1.32$. Within this model, this ratio is significantly smaller with respect to the experimental value of $H_{c2}/H_{c1} = 2.13$ corresponding to a value of 0.21 for r. This discrepancy finds probably its origin into the too small used supercell which does not allow us to determine explicitly the energy of the $M_S/3$ configuration, this energy being essential for an accurate description of the plateau.

In a very recent paper, Kim *et al.*[13] have done a similar investigation: they have found that $J_2^{\text{eff}}/J_1^{\text{eff}} = J_3/J_1 = j_3/(2j_1) = 0.21$ and $J_2^{\text{eff}}/J_3^{\text{eff}} = J_3/J_2 = j_3/(2j_2) = 1$, whereas we get $j_3/(2j_1) = 0.65$ and $j_3/(2j_2) = 4.5$.[23] Because they do not give too much detail on the determination of the coupling values and because the absolute values of J_i are not reported, it is difficult to analyze the origin of this discrepancy.

In order to have information on the orientation of the Co magnetic moments with respect to the axes of the α-CoV_2O_6 crystalline structure, we have analyzed, for the FF case into the smallest cell, the angular dependence of the magnetic moment into the ac plane by varying the angle β_{ac} of the quantization axis relative to the a direction. This is done by taking the spin-orbit coupling into account into the FLEUR

TABLE IV. Total-energy differences relative to the ground state obtained from the electronic-structure calculations E_{ES}-$E_{\text{ES}}(AA)$ and with the Ising model E_{Ising}-$E_{\text{Ising}}(AA)$ for the four considered configurations.

Order	E_{ES}-$E_{\text{ES}}(AA)$ (meV/f.u.)	E_{Ising}	E_{Ising}-$E_{\text{Ising}}(AA)$
AA	0.00	$-2j_1 + 2j_2 - j_3$	0
AF	0.72	$-2j_1 - 2j_2 + j_3$	$-4j_2 + 2j_3$
FA	1.22	$2j_1 - 2j_2 - j_3$	$4j_1 - 4j_2$
FF	2.35	$2j_1 + 2j_2 + j_3$	$4j_1 + 2j_3$

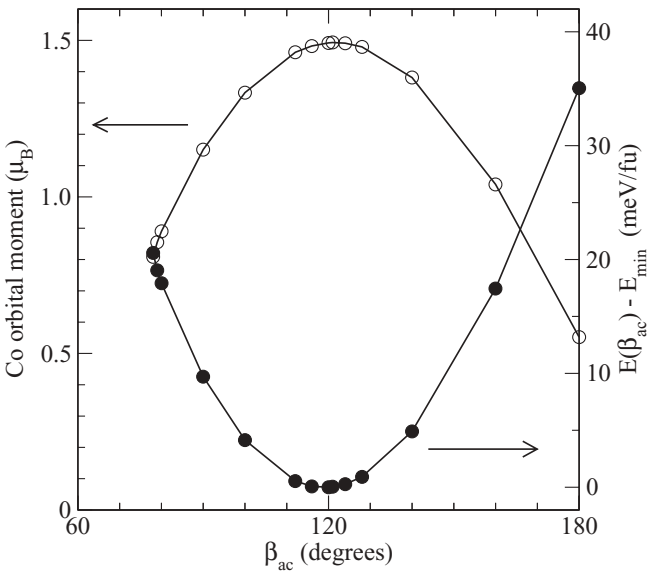

FIG. 8. Orbital moment on the Co atoms (open symbol) and total energy per formula unit (filled symbol) obtained for the ferromagnetic solution as a function of the β_{ac} angle of the quantization axis relative to the a direction.

calculations in a self-consistent way. A large orbital moment on the Co atoms is obtained reaching a value of 1.5 μ_B for $\beta_{ac} = 120^\circ$ corresponding to the energy minimum (Fig. 8) (the Co orbital moment being equal to 0.19 and 0.02 μ_B when the quantization axis is, respectively, set along the a and b directions). This direction is very close to the direction of the axis of the octahedron surrounding the Co atoms which is equal to 121° and agrees well with the value found by neutron diffraction (121.4°). These results lead us to the conclusion that the *ab initio* investigation predicts a total magnetic moment of 4.5 μ_B per Co atom directed along its CoO_6 octahedron axis in very good agreement with our neutron diffraction results.

IV. CONCLUSION

In conclusion, we characterized the magnetic structure of α-CoV_2O_6, in its ground and field-induced ordered states, and successfully correlated it to *ab initio* calculations. The neutron diffraction measurements indicated that in the ground state the order is ferromagnetic inside the chains along the b axis and antiferromagnetic between the chains (along the a and c axes). The antiferromagnetic interaction is characterized by a Néel temperature of about 14 K. The different distances between Co atoms in the ac plane lead to triangular frustrations responsible for the magnetization plateaux observed in the MH curves. The field-induced ferrimagnetic and ferromagnetic ordered states could be also characterized by neutron diffraction. The ferrimagnetic state is described by the $(\frac{2}{3},0,\frac{1}{3})$ propagation vector in the $C1$ space group and corresponds to an up-up-down configuration of the Co magnetic moments of the chains along the a and c directions. For all structures, the magnetic moments lie in the ac plane, along the axis of the CoO_6 octahedra, at an angle of 9.3° with respect to the c direction. The magnetic order and the interactions between the Co ions are in good agreement with the theoretical model. The magnetic configuration is confirmed by the Ising model on a triangular lattice with frustrated antiferromagnetic couplings between neighbor pairs of sites. The explicit determination of the total energy for various magnetic orders has allowed determining the interactions between the Co ions and has shown only a qualitative agreement with the data derived from magnetization measurements. The orientation of the magnetic moments was found close to the c direction, in agreement with the neutron diffraction data, and was evidenced by introducing the spin-orbit coupling in the model. This allowed us as well to estimate the orbital magnetic moment per Co atom to 1.5 μ_B, very close to the experimental value. Finally, a complete picture of the magnetic properties of α-CoV_2O_6 using both neutron diffraction measurements and theoretical calculations could be obtained.

ACKNOWLEDGMENT

This work was carried out under the framework of the MAD-BLAST project supported by the French Agence Nationale de la Recherche (ANR) under the reference ANR-09-BLAN-0187-03.

*Present address: Stephenson Institute for Renewable Energy & Department of Physics, University of Liverpool, UK.
†colis@ipcms.u-strasbg.fr

[1] S. Ishiwata, I. Terasaki, F. Ishii, N. Nagaosa, H. Mukuda, Y. Kitaoka, T. Saito, and M. Takano, Phys. Rev. Lett. **98**, 217201 (2007).
[2] R. Moubah, S. Colis, C. Ulhaq-Bouillet, M. Drillon, and A. Dinia, J. Mater. Chem. **18**, 5543 (2008).
[3] Z. He, J. I. Yamaura, Y. Ueda, and W. Cheng, J. Am. Chem. Soc. **131**, 7554 (2009).
[4] S. Yuasa, T. Nagahama, A. Fukushima, Y. Suzuki, and K. Ando, Nat. Mater. **3**, 868 (2004).
[5] H. Muller-Buschbaum and M. Kobel, J. Alloys Compd. **176**, 39 (1991).
[6] B. Jasper-Tönnies and H. K. Muller-Buschbaum, Z. Anorg. Allg. Chem. **508**, 7 (1984).
[7] K. Singh, A. Maignan, D. Pelloquin, O. Perez, and Ch. Simon, J. Mater. Chem. **22**, 6436 (2012).
[8] M. Lenertz, J. Alaria, D. Stoeffler, S. Colis, and A. Dinia, J. Phys. Chem. C **115**, 17190 (2011).
[9] S. A. J. Kimber, H. Mutka, T. Chatterji, T. Hofmann, P. F. Henry, H. N. Bordallo, D. N. Argyriou, and J. P. Attfield, Phys. Rev. B **84**, 104425 (2011).
[10] M. Markkula, A. M. Arevalo-Lopez, and J. P. Attfield, J. Solid State Chem. **192**, 390 (2012).
[11] M. Markkula, A. M. Arevalo-Lopez, and J. P. Attfield, Phys. Rev. B **86**, 134401 (2012).
[12] X. Yao, J. Phys. Chem. A **116**, 2278 (2012).
[13] B. Kim, B. H. Kim, K. Kim, H. C. Choi, S. Y. Park, Y. H. Jeong, and B. I. Min, Phys. Rev. B **85**, 220407(R) (2012).
[14] S. A. J. Kimber and J. P. Attfield, Phys. Rev. B **75**, 064406 (2007).
[15] S. Agrestini, L. C. Chapon, A. Daoud-Aladine, J. Schefer, A. Gukasov, C. Mazzoli, M. R. Lees, and O. A. Petrenko, Phys. Rev. Lett. **101**, 097207 (2008).
[16] R. Moubah, S. Colis, C. Ulhaq-Bouillet, M. Drillon, and A. Dinia, J. Phys.: Condens. Matter **23**, 276002 (2011).
[17] K. Mocała, J. Ziółkowski, and L. Dziembaj, J. Solid State Chem. **56**, 84 (1985).
[18] FLEUR is an implementation of the full potential linearized augmented plane wave method freely available at http://www.flapw.de funded by the European Research Network Ψ_k and managed by S. Bluegel.
[19] W. E. Pickett, Phys. Rev. Lett. **79**, 1746 (1997).
[20] H. Wu, M. W. Haverkort, Z. Hu, D. I. Khomskii, and L. H. Tjeng, Phys. Rev. Lett. **95**, 186401 (2005).
[21] D. Stoeffler and S. Colis, J. Phys.: Condens. Matter **17**, 6415 (2005).
[22] The total-energy difference between the AF and the FF configurations can be determined into a unit cell containing only two f.u. which allows us to perform accurately the calculation taking the spin-orbit coupling into account: it has confirmed that, for a given quantization axis, the FF-AF total-energy difference does not change (within the error bar of the calculation) when the spin-orbit coupling is introduced.
[23] Please keep in mind that J_j^{eff}, J_j, and j_j are the notations used for the couplings by Kim *et al.* (Ref. 13), Yao (Ref. 12), and calculated in our work, respectively.